

Determination of the Second-Order Rate Constant for the Reduction of Dopamine Quinone with Ascorbic Acid

David Sopchak and Barry Miller*

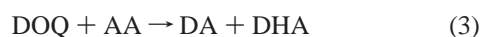
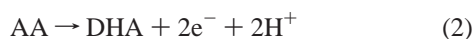
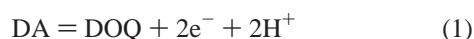
Department of Chemistry, Case Western Reserve University, Cleveland, Ohio 44106-7078

Received: March 22, 2000; In Final Form: May 31, 2000

The voltammetric determination of dopamine in the presence of ascorbic acid is strongly dependent on the local transport conditions because of the reduction of the product quinone with the ascorbate. Rotating ring-disk electrodes (RRDE) may be applied both to the kinetics of this system and to analytical advantage in detecting trace amounts of ascorbate. In the present work, RRDE techniques were used to determine the rate constant by which oxidized dopamine, generated at the disk, was reduced by ascorbate present in solution. This was accomplished by comparing the current generated at the ring by reduction of unreacted dopamine quinone to the amount predicted by theory for an infinitely fast reaction rate. Rate constants were obtained for ascorbate concentrations from 100 to 400 μM and dopamine concentrations from 2 to 10 mM using three different electrodes. A second-order rate constant of $1.5 \times 10^6 \text{ M}^{-1} \text{ s}^{-1}$ was found.

Introduction

The homogeneous reduction of the oxidized form of dopamine (DA), dopamine quinone (DOQ), by ascorbate (AA) is a well-known phenomenon which must be recognized in analytical methods, due to the extremely important biological pairing of DA and AA. While AA is thermodynamically easier to oxidize than DA, its oxidation at most electrode surfaces is normally found to be slower than that of DA. Both molecules are present in mammalian nerve and brain tissues. Often, AA is present at concentrations that are several orders of magnitude higher than DA, casting the DA which is present into a largely catalytic role of homogeneous charge transfer between any electrode being used for DA detection and the AA in solution.



DHA represents dehydroascorbate, the oxidized form of ascorbic acid.

It has long been recognized that the details of transport at electrodes are essential in designing single-electrode systems for DA monitoring to offset the effect of the catalytic regeneration of DA by the second-order reaction on analytical calibration. Various methods have been used^{1–3} to exclude signal enhancement from direct-electrode oxidation of AA, such as coating the electrode surface with a suitable material to prevent AA from reaching the electrode surface. An example of such a technique is coating the electrode with a thin film of Nafion.¹ The negatively charged sulfonate groups on the Nafion membrane repel negatively charged species such as AA, but allow DA to migrate across to the electrode surface. Such methods do not stop the catalytic enhancement of signal due to DA regeneration by AA in solution.

Microelectrodes have been employed in an effort to reduce the interaction of DOQ diffusing out from the electrode surface, reacting with AA in solution, and returning to the electrode during the time scale of the measurement. Early experiments⁴ resulted in the catalytic enhancement of the DA oxidation signal being lowered by a factor of 5. More recent experiments⁵ using both microelectrodes and high-pass filtering resulted in similar rejection of the catalytic signal enhancement. These methods are clearly an improvement over straightforward techniques. Living systems present still more challenges for microelectrodes relative to DOQ/AA interactions. It has been demonstrated⁶ that physical microelectrodes can behave in many different ways, depending on the sample volumes and time scales used for the measurement. A physically small electrode may not necessarily be an electrochemically small one.

Methods that remove AA from the immediate environment of the electrode, such as using a mesh impregnated with ascorbate oxidase above the working electrode,⁷ show promise at this time. This approach could attack the DA/AA interaction problem at its source by removing AA from the electrode environment.

Recently, we tested boron-doped-diamond (BDD) and tetrahedral-amorphous carbon, incorporating nitrogen electrodes (taC:N) for DA detection.⁸ The latter significantly improves the definition of the wave over BDD by relatively faster kinetics with the DA/DOQ couple yet higher overpotential for electrolyte oxidation. Unfortunately, while detection limits in phosphate-buffered saline (PBS) were very good, interference with AA renders simple detection by rotating disk electrode (RDE) methods infeasible. In an effort to separate out the DA component of the signal, we used the RRDE. AA oxidizes irreversibly to DHA, while DA can be oxidized and re-reduced easily within short time scales. The occurrence of reaction 3, however, turns this ring-current method into a better procedure for AA analysis than for DA.⁸

Kinetic Theory and Experiment. Albery et al. pioneered RRDE techniques for diffusion-layer titrations and expanded this to methods for the determination of kinetic-rate constants of first- and second-order reactions.^{9–12} Both diffusion-layer titration and kinetics techniques involve electrochemically

* To whom correspondence should be addressed. E-mail: bxm22@po.cwru.edu. Fax: (216) 368-3006.

generating one of the reacting species, B, at the disk, while the other species, A, which is electrochemically inactive at the disk potential, is present in solution. A homogeneous reaction between the two species occurs in solution, and depending on the rate at which B is being generated at the disk, some B can make it as far as the ring and can be detected by the reverse reaction that created it at the disk. At the boundary of the B-dominated region, created at the disk electrode, and the A-dominated region (the bulk of solution) exists a surface at which the concentrations of both species would be zero, because at that front there is just enough A to react with the B generated at the disk to remove both species.

It is important to point out that in our experiments, species A, ascorbic acid, is not electrochemically inactive. It will be made clear in this paper that this is not an obstacle in applying these methods to this system.

For the following equations, in RRDE geometry, r_1 is the disk electrode radius, and r_2 and r_3 are the inner and outer radii of the ring electrode, respectively. Albery⁵ has derived equations for locating the reaction front. For our purposes, we only need consider where that reaction front is in relation to the surface of the RRDE. The reaction front can be considered to be normal to the electrode surface. If this reaction front has a radius of exactly r_2 , and the reaction is infinitely fast, the ring current would be zero, because not enough B is generated in this case to reach the ring electrode for detection. The disk current at which the reaction front is at r_2 is given by

$$-i_d = M/[1 - F(\alpha)] \quad (4)$$

where

$$F(\alpha) = \frac{3^{1/2}}{2\pi} \int_0^\alpha \frac{dx}{x^{2/3}(1+x)} \quad (5)$$

$$\alpha = (r_2^3 - r_1^3)/r_1^3 \quad (6)$$

and

$$M = \pi r_1^2 n F D^{2/3} (0.510)^{1/3} \omega^{1/2} \nu^{-1/6} A / 3^{1/3} \Gamma(4/3) \quad (7)$$

F and n have the usual electrochemical meanings, D is the diffusion coefficient of species A, ω is the rotation speed, ν is the kinematic viscosity of the solution (taken as 0.010 cm²/s in this case) and A is the molar concentration of A in the bulk of solution. The integral in eq 2 can be solved directly and gives

$$F(\alpha) = \frac{3^{1/2}}{4\pi} \ln \frac{(1 + \alpha^{1/3})^3}{1 + \alpha} + \frac{3^{1/2}}{2\pi} \tan^{-1} \left(\frac{2\alpha^{1/3} - 1}{3^{1/2}} \right) + \frac{1}{4} \quad (8)$$

Because no reaction is infinitely fast, the reaction front has a finite thickness. Some A is able to penetrate further into the B-dominated region and vice versa. This reaction-front thickness is inversely proportional to the rate constant of the reaction of A and B. For RRDEs with r_3 large enough to collect all the B that survives crossing this reaction front, the rate constant can be determined by determining the "kinetic" collection efficiency of the electrode, N_k , where

$$N_k = i_{r,k} / -i_{d,k} \quad (9)$$

$i_{d,k}$ is defined above in eq 4, and $i_{r,k}$ is the ring current obtained when the disk current is $i_{d,k}$. Following Albery,¹²

$$N_k = 0.339 r_2^2 r_1^{-2} D^{1/3} \nu^{-1/3} [1 - F(\alpha)] \omega (kA)^{-1} \quad (10)$$

TABLE 1

RRDE electrodes	radius (cm)		
	r_1	r_2	r_3
graphite/graphite	0.237	0.259	0.320
Au/Au	0.220	0.262	0.323
Pt/Pt	0.237	0.260	0.309

Rearranging and substituting,

$$k = 0.339 r_2^2 r_1^{-2} D^{1/3} \nu^{-1/3} [1 - F(\alpha)] \omega (-i_{d,k}) (i_{r,k} A)^{-1} \quad (11)$$

This approach was first used⁵ to determine the rate constant for the oxidation of allyl alcohol by Br₂ generated at the disk from Br⁻. In that experiment, allyl alcohol was the nonelectrochemically active species, A.

Experimental Section

Ultrapure water (> 18.3 MΩcm) and reagent-grade chemicals were used to make the PBS buffer (2.68 mM KCl, 1.47 mM KH₂PO₄, 68.44 mM NaCl, 4.03 mM Na₂HPO₄). Dopamine hydrochloride and ascorbic acid (Aldrich) were used without further purification.

Electrodes used were graphite/graphite, gold/gold and platinum/platinum RRDEs. All electrodes were fabricated in our laboratory by brazing the metals or attaching the graphite using silver epoxy to steel rods and tubes, machining to the desired dimensions, nesting the rod inside the tube, potting with epoxy (Shell Chemical, Epon 862, and Epi-Cure 2259), and finally, machining and polishing the electrode surfaces to a 3-μm alumina finish. Dimensions of the electrodes were measured with a binocular microscope and micrometer stage and are listed in Table 1.

Procedure. Solutions were made up as follows: dopamine hydrochloride was used in concentrations of 1, 2, and 5 mM and ascorbic acid, at 100, 200, and 400 μM. All solutions were used within 2 h of preparation, purged with N₂ for at least 10 min prior to the experiment and held under an N₂ blanket for the duration of the experiment. In all rate constant determinations, the disk electrode was galvanostatically controlled and scanned or held at $i_{d,k}$ while the ring electrode was potentiostatically held at a potential for limiting current detection of DOQ. Data acquisition and control was through a National Instruments PCI-1200 data acquisition card and LabView software, in conjunction with a Pine AFCBP1 Bipotentiostat. All experiments were run at ambient temperature, 21 ± 2 °C.

Results and Discussion

Experiments were initially conducted with the disk held at a potential to give a limiting current for both AA and DA oxidation at the disk, and the ring was held at a potential sufficient to reduce the DOQ back to DA. These experiments did not separate out the DA contribution to the disk signal. On the contrary, the DOQ generated at the disk electrode was so quickly reduced in an environment of about half equimolar or higher AA, depending on the geometry of the particular RRDE used, that none of it reached the ring for detection, as seen in Figure 1. The sensitivity of the ring current to low levels of AA made this experiment more desirable for detecting small amounts of AA in the presence of DA.⁸ While this phenomenon negates discrimination of a small DA signal in the presence of AA, RRDE methods allow for further quantitative exploration of the DOQ/AA interactions, as described earlier.

The diffusion coefficient of AA was separately determined for this experiment from Levich behavior and found to be 4.7 × 10⁻⁶ cm²/s.

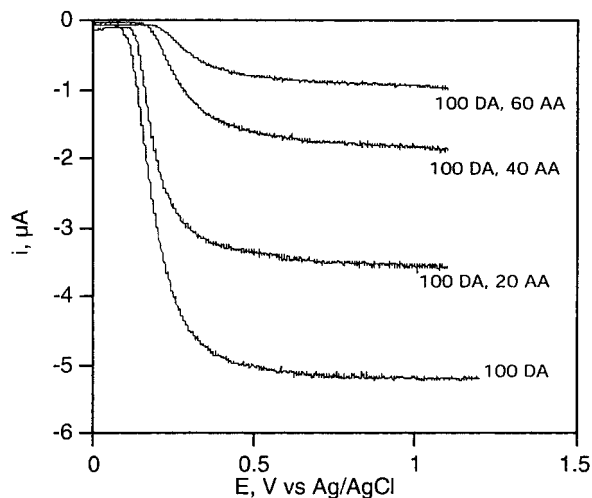


Figure 1. Ring currents at a Pt/Pt RRDE for 100 μM DA with 0–60 μM AA in PBS. Ring potential was held at 0.0 V vs Ag/AgCl, and the disk potential was scanned as indicated. Scan rate was 10 mV/s; 168 rad/s, rotation speed.

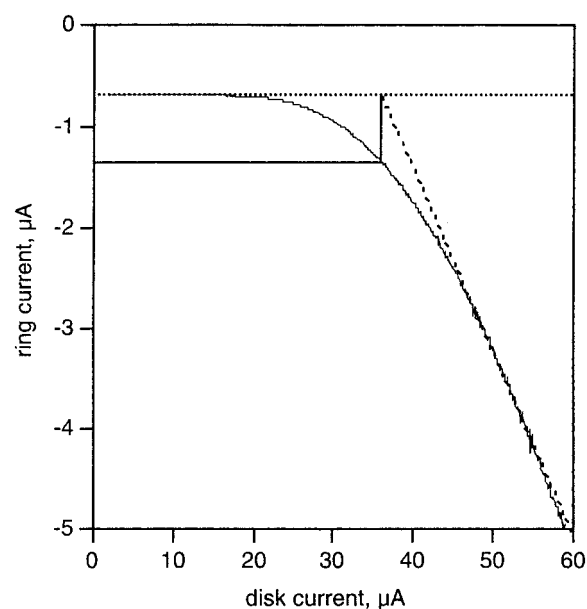


Figure 2. Plot of ring vs disk currents for an HOPG/graphite RRDE in 2 mM DA/100 μM AA. 168 rad/s rotation speed, 5 mV/s scan rate. Horizontal dotted line is the baseline current; diagonal dashed line, theoretical ring current behavior with infinitely fast kinetics (slope $-N_{id}$); vertical solid line, “kinetic” disk current $i_{d,k}$; and horizontal solid line, “kinetic” ring current, $i_{r,k}$.

All scans had a background ring current of less than 1 μA . This current was present even in solutions containing only PBS. The current was rotation-speed invariant and reproducible over the course of an experiment and was subtracted in all ring-current data used for computing kinetic parameters.

The rate constant of the reaction can be obtained from the disk current scans with a potentiostatted ring either graphically or numerically. Although all results reported in this paper were calculated numerically from eqs 1 and 8, the graphic method better illustrates the kinetic behavior of the system. Figure 2 shows a typical scan. The ring current starts out at a constant (the background current) and grows more cathodic as the reaction front of the DOQ advances to r_2 . As the reaction front moves past r_2 , the ring current increases to $-N_{id}$, the collection efficiency of the electrode times the disk current, and follows this behavior.

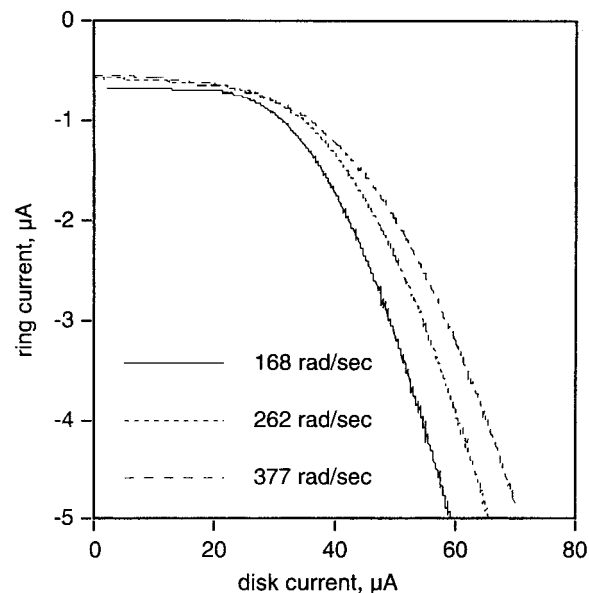


Figure 3. Plot of ring current vs disk current for an HOPG/graphite RRDE in 2 mM DA/100 μM AA at 168, 262, and 377 rad/s rotation speed, 5 mV/s scan rate.

TABLE 2

[DA], mM	[AA], μM	k , $\text{M}^{-1} \text{s}^{-1}$	no. of runs used, as in Fig 2
2	100	1.4×10^6	6
5	100	1.5×10^6	8
10	100	1.4×10^6	3
5	200	1.6×10^6	20
5	400	1.5×10^6	16

For an infinitely fast reaction, the ring current would track the baseline current and then follow the diagonal dashed line in Figure 2, because the reaction front would have no radial depth and would cross r_2 at one discrete i_d . The point at which the diagonal line crosses the baseline gives $i_{d,k}$. Taking the ring current at this point and subtracting out the baseline current gives $i_{r,k}$. Substituting these values into eq 8 yields the second-order rate constant.

At higher rotation speeds, the reaction-front thickness increases along the radial dimension, and the DOQ generated at the disk gets reduced back more readily, owing to the shrinking hydrodynamic boundary layer and greater fluid flow across the electrode, as illustrated in Figure 3. Note that all curves finally achieve identical slopes of $-N_{id}$, but the curves at higher rotation speeds are displaced toward greater disk currents, as predicted by theory.

A summary of the second-order rate constants is given in Table 2.

From all data over a 5-fold concentration range in DA and a 4-fold range in AA, k was found to be $1.5 \pm 0.4 \times 10^6 \text{ M}^{-1} \text{ s}^{-1}$. Thus, changing the DA or AA concentration had no measurable effect on the rate constant.

Using measurements of current transients at microelectrodes, Dayton⁴ et al. determined a rate constant for this reaction of $3.2 \times 10^5 \text{ M}^{-1} \text{ s}^{-1}$. Earlier experiments by Tse¹³ et al. put a rough lower limit on this rate constant, reporting a pseudo-first-order value of ca. $> 3 \times 10^2 \text{ s}^{-1}$. As can be seen above, our results are within an order of magnitude of the results reported by Dayton.

A major difference between RRDE methods and chronoamperometry is the steady-state nature of the RRDE method, whereas chronoamperometry with microelectrodes is based on

transient signals. It has yet to be shown which method is more accurate for the characterization of this system.

We referred earlier to a difference in our situation at variance to the Albery-Bruckenstein model. Normally, diffusion-layer titrations are carried out with one species that is not electroactive at the disk potential. This is not the case in our study because AA is electroactive at the disk. In actuality, AA is thermodynamically easier to oxidize than DA, but in practice, the overpotentials of these two compounds reverse this effect. At the potential range required to generate the disk currents in these experiments, less than 10% of the current at the disk can be directly attributed to AA. Along with the fact that AA and DA have almost the same diffusion coefficients, the question of whether AA near the disk was oxidized by DA or the disk itself is rendered moot.

References and Notes

(1) Gerhardt, G. A.; Oke, A. F.; Nagy, G.; Moghaddam B.; Adams R. N. *Brain Res.* **1984**, *290*, 390.

(2) Pihel, K.; Walker, Q. D.; Wightman, R. M. *Anal. Chem.* **1996**, *68*, 2084.

(3) Dalmia, A.; Liu, C. C.; Savinell, R. F. *J. Electroanal. Chem.* **1997**, *430*, 205.

(4) Dayton, M. A.; Ewing, A. G.; Wightman, R.M. *Anal. Chem.* **1980**, *52*, 2392.

(5) Cahill, P. S.; Walker, Q. D.; Finnegan, J. M.; Mickelson, G. E.; Travis, E. R.; Wightman, R. M. *Anal. Chem.* **1996**, *68*, 3180.

(6) Kashyap R.; Grätzl, M. *Anal. Chem.* **1998**, *70*, 1468.

(7) Pariente, F.; Tobalina, F.; Moreno, G.; Hernandez, L.; Lorenzo, E.; Abruna, H. D. *Anal. Chem.* **1997**, *69*, 4065.

(8) Sopchak, D.; Miller, B.; Kalish, R.; Shi, X. manuscript in preparation.

(9) Albery, W. J.; Bruckenstein, S.; Johnson, D. C. *Trans. Faraday Soc.* **1966**, *62*, 1938.

(10) Albery, W. J.; Bruckenstein, S. *Trans Faraday Soc.* **1966**, *62*, 1946.

(11) Albery, W. J.; Bruckenstein, S. *Trans Faraday Soc.* **1966**, *62*, 2584.

(12) Albery, W. J.; Hitchman, M. L.; Ulstrup, J. *Trans Faraday Soc.* **1969**, *65*, 1101.

(13) Tse, D. C. S.; McCreery, R. L.; Adams, R. N. *J. Med. Chem.* **1976**, *19*, 37.